

Plant halides as potential norovirus 3CLpro inhibitors: An *in silico* approach

Muskan Sharma¹, Gourav Choudhir², Sakshi Sharma², Nikunaj Bhardwaj³, Abhay Tiwari⁴ & Sushil Kumar^{2*}

¹Department of Bioscience and Biotechnology, Banasthali Vidyapith, Vanasthali Road, Dist- Tonk-304 022, Rajasthan, India

²Department of Botany, Chaudhary Charan Singh University, Meerut-250 004, Uttar Pradesh, India

³Department of Zoology, Maharaj Singh College, Saharanpur-247 001, Uttar Pradesh, India

⁴Department of Biotechnology, School of Engineering & Technology (SET), Sharda University, Knowledge Park III, Greater Noida-201 310, Uttar Pradesh, India

Received 09 May 2025; revised 18 May 2025

Norovirus, a member of Caliciviridae causes severe gastroenteritis in all phases of human life. Norovirus is a major global cause of acute gastroenteritis with high mortality in children and immunocompromised individuals. The norovirus 3CL protease (3CLpro) is a cysteine protease that post-translationally cleaves ORF1 (open reading frame 1)-encoded polyproteins into six non-structural proteins (nsPs). These nsPs p48, NTPase, p22, VPg, Pro, and Pol are essential for the replication and transcription of the viral genome hence 3CLpro is inevitable for norovirus multiplication. The indispensable role multiplication and conserved nature of 3CLpro makes it an attractive target for anti-norovirus therapeutics. Currently there is no approved drug or vaccine against norovirus. In the current investigation, an *in silico* approach has been employed to find lead halide secondary metabolite from higher plants against 3CLpro. The library of 66 halide plant metabolites from terrestrial habitats has been screened for drug likeliness and ADME qualified 36 molecules were subjected to molecular docking. The molecule, gravacridonechlorine in complex with 3CLpro exhibited the highest binding affinity (-6.9 kcal/mol) and validated through MD simulation and MMPBSA (ΔG_{bind} -134.142 kJ/mol). The findings concluded that the gravacridonechlorine-3CLpro complex is favoured energetically and can be a suitable inhibitor for norovirus.

Keywords: Free energy, Gravacridonechlorine, Non-structural proteins, Pharmacodynamics, Pharmacokinetics

Norovirus, belonging to the family of *Caliciviridae* is an RNA virus that causes morbidity due to acute gastroenteritis (AGE) in all age groups. Human norovirus is a major contributor to AGE. The virus is known for its diversity and is also addressed as a "shape shifter" because of its property to escape population immunity as new virus variants emerge every 2-4 generations¹. It is chiefly divided into ten genotypes from genotype I (GI) to genotype 10 (GX) which further divided into more than 40 sub-genotypes based on phylogenetic analysis. Humans are mainly infected by GI, GII, and GIV, subdivided into 9, 19, and 1 genotypes, respectively². The majority of outbreaks and sporadic cases worldwide are caused by GII.4. In Asia norovirus new genotypes GII.P17 to GII.17 are prevalent³. The global trends of norovirus outbreaks as per the Centre for Disease Control and Prevention, state that annually ~685 million cases are caused by norovirus worldwide. Among them, 200 million cases are reported in

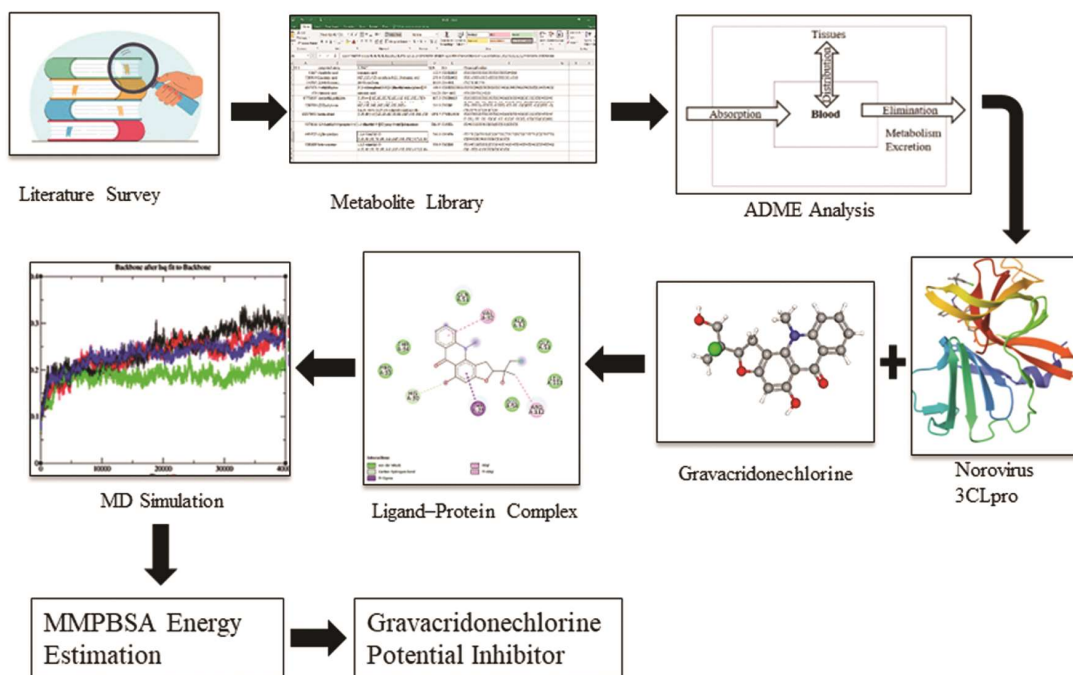
children below 5 years. This leads to an estimated death of 50,000 children every year, the majority of whom belong to developing countries. A total cost of 60 billion USD is consumed for norovirus-related healthcare purposes. The norovirus outbreaks are generally observed during the cooler months of November to April (Centre of Disease Control and Prevention, <https://www.cdc.gov/norovirus/burden> Last visited 20th Dec. 2024).

Norovirus is highly contagious and can spread through contact with vomit, feces, contaminated food, water, and surfaces⁴. Food borne transmission itself accounts for 7% of the disease³. The virus exhibits broad temperature tolerance and can remain infectious for days, maintaining its pathogenicity. The seasonal pattern of norovirus AGE outbreaks in northern and southern hemispheres shows a higher incidence between November and April and May to September, respectively. Due to the lack of substantial cell culture systems and suitable animal models the mechanism of human norovirus is not fully known⁵. Following infection, symptoms of AGE such as nausea, abdominal cramps, vomiting, and diarrhea typically

*Correspondence:

E-mail: skg1979@gmail.com

Suppl. data available on respective page of NOPR



Graphical abstract

appear within 24 to 48 h⁶. Intestinal epithelial cells and immune cells such as dendritic cells and macrophages are primary targets for norovirus. Human noroviruses use the immunogenic P2 domain of their VP1 protein to bind HBGAs (glycans) on mucosal epithelial cells. Norovirus infection induces histological changes such as microvilli shortening, villi blunting, mitochondrial alterations, cytoplasmic vacuolization, intercellular edema, crypt hyperplasia, and epithelial barrier disruption. Villi shortening reduce enteric enzyme activity, leading to diarrhoea, while delayed gastric emptying due to altered gastric motor function likely causes vomiting and nausea. Viral shedding continues in the feces of symptomatic and asymptomatic infected persons⁵.

Positive sense ssRNA of approximately 7 kb long build norovirus genome. The expression of the genome occurs in the form of three polycistronic reading frames named ORF1, ORF2, and ORF3. Two major capsid polyproteins VP1 and VP2 of about 200 kD are encoded by ORF2 and ORF3, respectively. The largest ORF in the viral genome encodes six nsPs, namely p48, NTPase, p22, VPg, Pro, and Pol. These proteins are essential for the replication and transcription of the viral genome^{1,7} (Fig. 1).

The norovirus 3CL protease (3CLpro) is a cysteine protease that post-translationally cleaves ORF1-encoded polyproteins into six non-structural proteins.

The crystalline 3D structure of 3CLpro shows chymotrypsin-like folds and has two domains. The highly conserved active sites of this enzyme possess a triad of Cys¹³⁹, His³⁰, and Glu⁵⁴ each working as the nucleophile, general acid/base, and deprotonating agent, respectively⁸. Together they form a binding cleft for specific substrate P1Gln (or Glu) residue. These six proteins are essential for norovirus replication. Norovirus with inactive 3CLpro cannot produce the necessary components to multiply within a host. This proves the necessity of 3CLpro in the life cycle of norovirus and makes it an attractive target for anti-norovirus therapeutics⁹. Synthetic inhibitors, including peptidyl transition state mimics, macrocyclic compounds, and oxazolidinone derivatives¹⁰, have shown significant potency *in vitro* and in some cases, efficacy in animal models. Natural products, particularly certain phytochemicals, have also demonstrated antiviral effects against protease¹¹. Structure-based drug design and computational methods have been instrumental in these efforts, providing valuable insights into the mechanisms of inhibition and guiding the development of more effective compounds¹⁰. He *et al.* (2022) screened 700 antiviral compounds against the 3CL protease active site and found Sorafenib, YM201636, and LDC4297 exhibited favorable binding. Despite these advancements, the lack of approved norovirus-

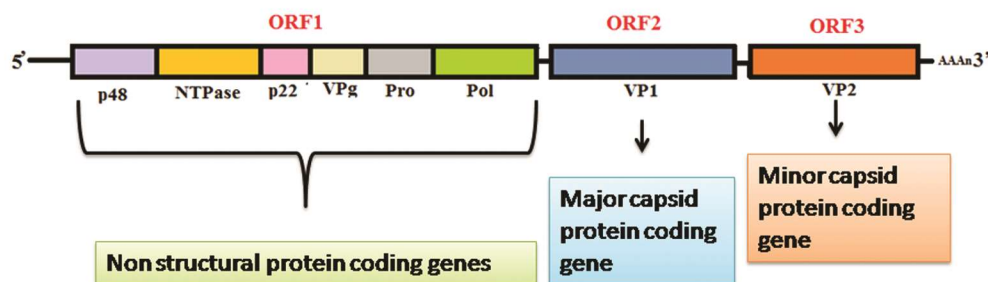


Fig. 1 — Genome of Norovirus with three open reading frames (ORFs)

specific antivirals underscores the continued need for focused research. Several attempts have been made to find promising inhibitors for 3CLpro to treat norovirus infections using pre-approved antiviral drug molecules using *in silico* approach¹² and rarely the new natural molecules. Because conventional drug molecule discovery needs more time, labour, and money¹³ authors used an *in silico* approach to screen a library of halogenated secondary metabolites from terrestrial plants against norovirus 3CLpro.

A great variety of halogenated drugs are doing well in the market pointing to the importance of halogenated compounds as drugs¹⁴. Among them, almost all are synthetic and rarely a drug with natural origin. Plant secondary metabolites consisting of halogens although have great potential to be effective drugs but not recognized to the extent they deserve. Compared to marine algae, halogenated secondary metabolites, are rare in angiosperms and other terrestrial plants but recently a number of these metabolites have been discovered in terrestrial flora^{15,16}. Blood-brain barrier (BBB) permeability is a significant criterion in drug development and can be enhanced by the addition of halogen atoms in drug molecules¹⁷. Halogenated compounds are increasingly used in new drugs. The use of halogen atoms in drugs improves the potency, selectivity, and metabolic stability of drugs. In 2021, the FDA approved 14 new drugs and all were halogenated. Thirteen new halogenated drugs were approved in 2020. The halogenated drugs generally contain fluorine and chlorine or their combination¹³. At present, no approved antiviral and vaccine are available against norovirus¹⁸. In this investigation, an *in silico* approach has been employed to find lead halogenated secondary metabolite from a library of metabolites for inhibiting viral 3CLpro activity to develop potent anti-norovirus therapeutics.

Materials and Methods

Library construction and ADME analysis

A diverse library of sixty six¹⁹ halide plant natural products was created from a comprehensive literature review and used in virtual screening to identify potential norovirus inhibitors^{20,21}. The PubChem Database was used to retrieve the chemical and structural characteristics of these metabolites, including their molecular weight, chemical formulae, and canonical SMILES²². The pharmacokinetic and pharmacodynamic features of a previously prepared library of halide phytomolecules from higher plants were set on by using Lipinski's rule²³ (Table S1). The web-based SwissADME tool was employed to ascertain the drug-likeness of all phytomolecules based on ADME properties²⁴. Halide metabolites that adhered to Lipinski's rule were selected for molecular docking studies.

Docking-ready ligand and protein

The three-dimensional structure of selected halide phyto-molecules was converted to pdb file format using canonical SMILES as input in the OpenBabel program. Before saving the structure to pdb file format hydrogen atoms that are explicitly represented were added. The reduction of the system's energy and optimization of selected halide phyto-molecules was carried out employing the Open Babel tool of PyRx and then saved as pdbqt file format²⁵.

RCSB database was used to retrieve 3-D crystal structure coordinates for norovirus 3CLpro (PDB ID 5E0J) (RCSB 2022). Using UCSF chimera, water, and groups other than amino acid residues were eliminated from the protein structure to carry out docking investigations²⁶. The module clean geometry of Discovery Studio was plied to carry out the optimization of the norovirus 3CLpro structure, which was then saved in pdb format. Later, using the MGL

tool introduction of polar hydrogen atoms and Kollman charges was done and resulted structure was saved in pdbqt file format²⁷.

Ligand-protein docking and MD simulation

AutoDock Vina was employed to dock halide phytometabolites to the 3CLpro protein to identify potential inhibitors²⁸. The grid box had the coordinates X=20.223, Y=1.321, and Z=-16.419 as its centre, and its dimensions were 16Å×16Å×16Å. The system's exhaustiveness was kept at 16. Other characteristics remained as defaults. The binding energies of selected phytometabolites ranged between -6.9 to -1.5 kcal/mol. The minimum binding energy observed for Gravacridonechlorine (PubChem CID-5315835) (Table S2 and Fig. S1) was selected to evaluate the stability and pharmacodynamic attributes of the Gravacridonechlorine-3CLpro complex. The interactions of Gravacridonechlorine and 3CLpro were drawn using Discovery Studio and visualized by PyMol²⁹.

The dynamic motions of the Gravacridonechlorine-3CLpro complex were evaluated through MD simulation studies that were performed employing GROMACS 5.1.4 suite³⁰, aided with force field GRMOS96 43a1. The PRODRG server was used to create a file that describes the structure and properties of a ligand³¹. Gravacridonechlorine-3CLpro complex was dissolved in a cubical box and the system was neutralized by attaching a suitable number of ions. The system's energy was lowered by repeatedly moving in the direction that caused the greatest decrease in energy. Steric collisions were restricted by maintaining a convergence requirement lesser than 1000 kJ/mol/nm. The Particle Mesh Ewald (PME) method was used to calculate the non-bonded interactions between Gravacridonechlorine and 3CLpro³² at the cut-off radius of 9 nm. There were two steps in the equilibration process. In the entrée step under NVT ensemble, during 100ps, the solvent and ions were not subject to control followed by under NPT ensemble, for 100ps, the constraint weight from the 3CLpro and Gravacridonechlorine-3CLpro complex was continuously reduced. The algorithm LINCS was applied to coerce the length of hydrogen and other bonds^{33,32}. To retain a constant pressure and temperature (1atm and 300K), Parrinello Rahman pressure coupling and Berendsen's thermostat were used throughout the simulation of the system³⁴. A molecular dynamics simulation was performed after the system had reached equilibrium, using the

LeapFrog integrator with a 2fs step size and periodic boundary conditions for 100ns. The MD simulation trajectory was evaluated using customized Python-3.5 scripts and the easy-to-access GROMACS tool³⁵.

Analysis of MMPBSA Energy

The binding energy (ΔG_{bind}) for the best pose of Gravacridonechlorine-3CLpro complex was subjected to further refinement and energy contribution for each residue was determined using MMPBSA. The electrostatic solvation energy (ΔG_{psolv}) was calculated using the Poisson-Boltzmann equation and the non-polar solvation energy (ΔG_{npolv}) was computed by applying a linear function of the solvent-accessible surface area (SASA)³⁶. Gravacridonechlorine-3CLpro complex's binding free energy components were determined using the *g_mmpbsa* module of GROMACS³⁷. For this assessment, the last 10ns of trajectory have been used.

Results and Discussion

Drug-likeness

In silico drug-like behavior of halide phyto-molecules from higher plants was determined based on size, lipophilicity, flexibility, bonding nature, electron distribution of phyto-molecules as well as ADME analysis. Out of sixty six, 36 halide phyto-molecules agreed with Lipinski's rule²³ have suitable pharmacophoric and pharmacokinetic attributes, and were selected for further *in silico* analyses to find the best norovirus inhibitory molecules (Table S1).

Molecular Docking and MD Simulations

The minimum binding energy (-6.9 kcal/mol) was exhibited by Gravacridonechlorine (PubChem CID-5315835), hence Gravacridonechlorine binding with 3CLpro was analyzed for its' non-covalent interactions with 3CLpro active site. X-ray crystallographic study revealed that residues Cys¹³⁹, His³⁰, and Glu⁵⁴ principally constitute the active site of norovirus 3CLpro⁸. Analysis of 2D Gravacridonechlorine-3CLpro complex using PyMol revealed van der Waals interactions with Pro³³, Thr³⁴, Gln⁵¹, Ala⁵², Gly⁵³, Glu⁵⁴, and Leu¹¹². The residue Glu⁵⁴ is among the most conserved residues and crucial for 3CLpro enzymatic activity. Such binding directly intervenes in the normal functioning of the enzyme. The presence of a carbon-hydrogen bond (C-H bond) between Gravacridonechlorine and His³⁰ is another positive finding. His³⁰ is another conserved residue in the active site, and this interaction might

further enhance the inhibitory potential of Gravacridonechlorine. These interactions could be particularly important for inhibiting a broad range of norovirus strains. The analysis also identified weaker interactions with residues like Arg¹¹² (alkyl), Thr²⁹ (π - σ), and Val³² (π -alkyl) located around the conserved residues in the active pocket. These interactions, while weaker, might contribute to the overall binding affinity and positioning of Gravacridonechlorine within the 3CLpro structure (Fig. 2).

The docking interactions provide compelling evidence for Gravacridonechlorine as a potential inhibitor of norovirus 3CLpro. The strong binding energy, interactions with key conserved residues in the active site (Glu⁵⁴ and His³⁰), and additional contacts around the pocket all suggest a mechanism by which Gravacridonechlorine could interfere with viral replication. This highlights Gravacridonechlorine as a promising lead for further investigation as a potential therapeutic agent against norovirus. Gravacridonechlorine is found in *Ruta graveolens*, a well-known plant in Homeopathy and Ayurveda used for the treatment of arthritis, rheumatic pains, ulcers,

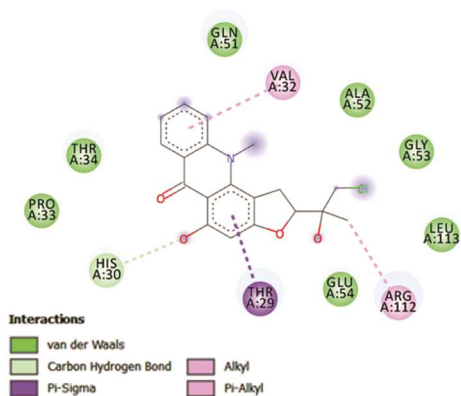


Fig. 2 —2D Interaction diagram of Gravacridonechlorine-3CLpro complex representing non-covalent interactions with residues in the active site in close vicinity of active site triad

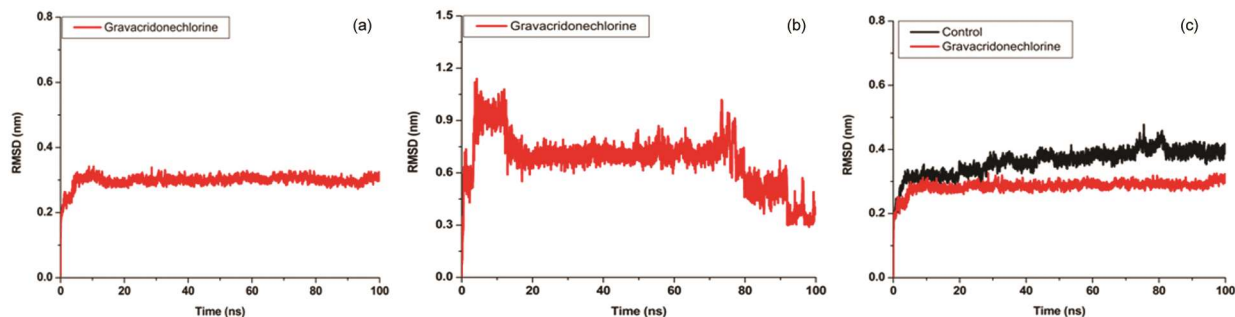


Fig. 3 —RMSD fluctuations over simulation time (a) Norovirus 3CLpro backbone; (b) Gravacridonechlorine ligand; and (c) Norovirus 3CLpro (control) and Gravacridonechlorine-3CLpro complex

eczema, the antidote for venoms, insect repellent, etc. Studies were also carried out for its anticancer potential³⁷.

Prediction of structural stability of Gravacridonechlorine-3CLpro complex through MD Simulations

Molecular docking results indicated that Gravacridonechlorine with the least binding energy and the highest affinity³⁸ could be the possible inhibitor of 3CLpro of norovirus. To validate docking results and assess complex stability, molecular dynamics (MD) simulations were performed. Ligand binding can induce conformational changes in proteins. Therefore, RMSD, RMSF, and Rg analyses were conducted on protein backbones and the complex to evaluate structural changes in 3CLpro upon Gravacridonechlorine binding.

Analysis of root mean square deviation

The C_α RMSD is a key attribute for assessing the average positional deviation of protein backbone atoms. This analysis can be applied to both protein backbones and ligand-protein complexes to evaluate conformational changes and complex stability during MD simulations. The time-dependent average RMSD of 3CLpro backbone in free and Gravacridonechlorine-3CLpro complex ranged between 0.20-0.30 nm attaining the plateau at 10 ns. The average RMSD of 3CLpro backbone and Gravacridonechlorine-3CLpro complex ranged ~0.285-0.298 nm, although the average RMSD of Gravacridonechlorine was recorded at 0.673 nm. Minor fluctuations in RMSD of free and bound states of 3CLpro indicate that there are no major conformational alterations in the two states and the interaction of Gravacridonechlorine does not significantly alter the protein's backbone structure (Fig. 3).

Analysis root mean square fluctuations

RMSF quantifies residue-level fluctuations around their average position, reflecting the dynamics of the

system. During the simulation period, the RMSF of 3CLpro and Gravacridonechlorine-3CLpro complex fluctuates from 0.125 to 0.102 nm, respectively (Fig. 4). Close examination of the RMSF graph revealed that Gravacridonechlorine interactions with residues 30-55 appear to stabilize the 3CLpro structure. In contrast, binding near residues 112-113 seems to induce slight flexibility, suggesting minor perturbations in the protein structure. Overall, the RMSF analysis indicates that Gravacridonechlorine binding does not cause significant alterations to the protein's native structure³⁹.

Analysis of protein compactness

Protein compactness is evaluated in the form of the radius of gyration (Rg). Lower Rg values indicate more stability of the protein. Since it is typical for ligand interaction to cause protein unfolding, Rg values were determined during the whole simulation. The Rg values of 3CLpro and Gravacridonechlorine-3CLpro complex were centered on ~1.49 nm and ~1.48 nm, respectively inferring that binding of Gravacridonechlorine to 3CLpro doesn't impart significant alteration in its compactness and integrity (Fig. 5). Initial interaction of Gravacridonechlorine with 3CLpro resulted in an increase in Rg values, suggesting an initial increase in protein structural flexibility upon binding. However, the system subsequently stabilized, and the Rg values converged to levels below those of the control, indicating a potential stabilization of the protein structure in the presence of Gravacridonechlorine.

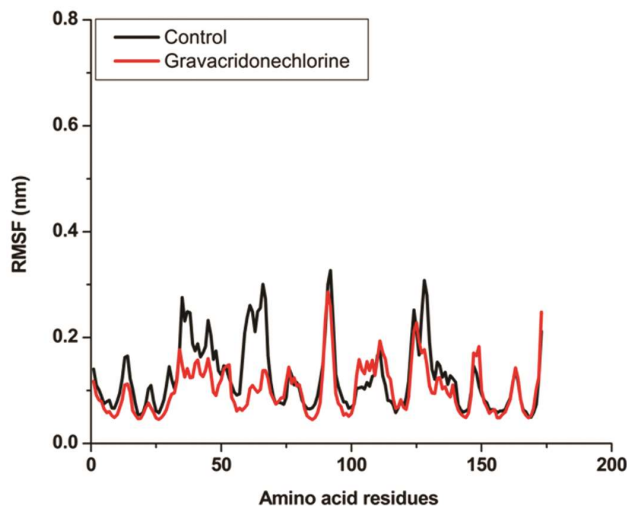


Fig. 4 —Comparative RMSF profiles of norovirus 3CLpro and Gravacridonechlorine-3CLpro complex representing residue level fluctuations

Analysis of solvent-accessible surface area

The hydrophobic amino acids of hydrophobic pockets remain protected from the aquatic surroundings due to hydrophobic interactions among these residues and stabilize the protein structure. Solvent-accessible surface area is meant to measure how easily accessible proteins are to solvents. It determines the free energy of salvation per atom of the system. Free 3CLpro, SASA profile showed the maxima at ~78.90 nm² which shifted for Gravacridonechlorine-3CLpro complex to ~79.13 nm² (Fig. 6) indicating no significant difference in the conformation of the protein after ligand binding.

The mean attribute values of the MD simulation are enumerated in (Table 1). Similar studies investigating Chikungunya virus, conducted by Kumar *et al.*

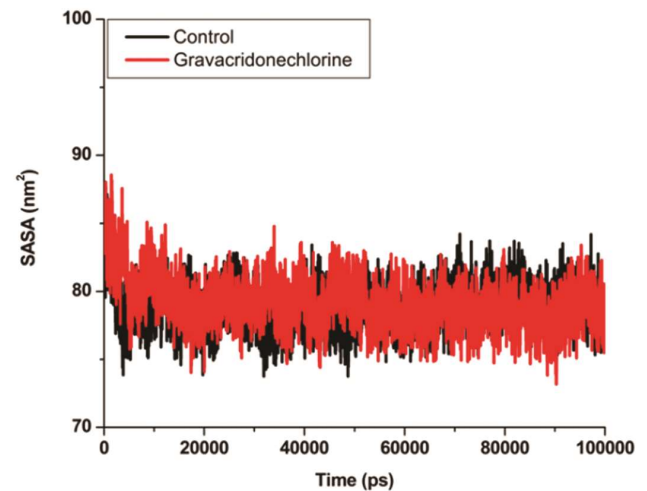


Fig. 5 —Comparative Rg profiles representing compaction pattern of norovirus 3CLpro and Gravacridonechlorine-3CLpro complex

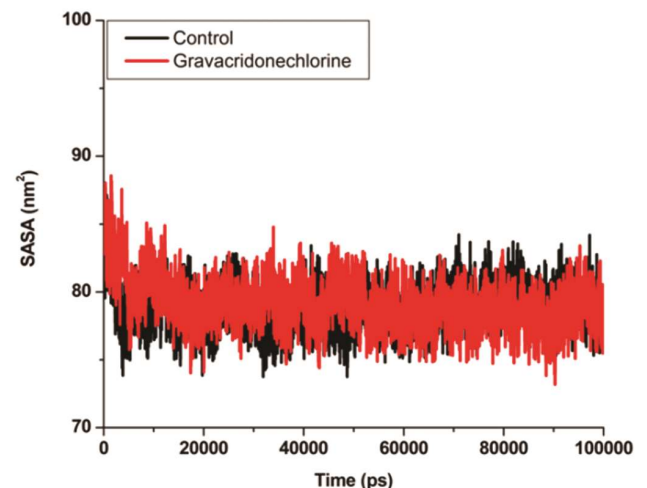


Fig. 6 —Solvent accessible surface area profile for control and Gravacridonechlorine-3CLpro complex

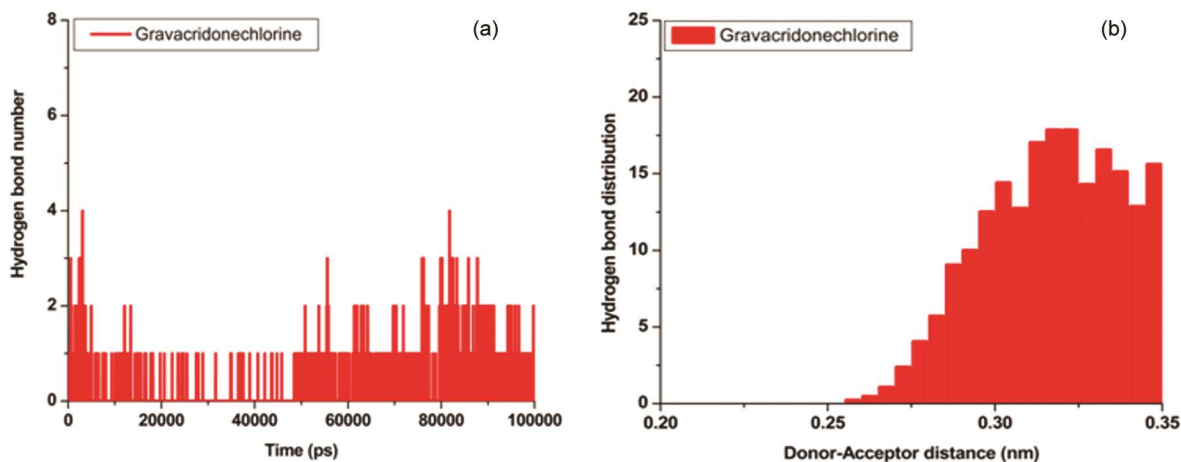


Fig. 7 —Number and distribution of hydrogen bonds between Gravacridonechlorine and 3CL pro during MD simulation length

Table 1 — Average values of MD simulation attributes

Parameter	Control	Gravacridonechlorine
Backbone RMSD	0.36275±0.03956	0.28533±0.01732
Complex RMSD	-	0.29843±0.01709
Ligand RMSD	-	0.67273±0.14545
RMSF	0.12529±0.063	0.10236±0.04668
Rg	1.4867±0.01202	1.47673±0.00994
SASA	78.89581±1.55683	79.13028±1.81195

(2024)²⁰, utilized the same library of halogenated plant secondary metabolites. Their research identified pipoxide chlorohydrin as a potential inhibitor of the nSP2pro.

Hydrogen bond analysis of Gravacridonechlorine-3CLpro complex

The H-bond between 3CLpro and halide metabolite Gravacridonechlorine was computed using the h_bond module of GROMACS. The hydrogen bond scattering was found all over the 100ns simulation period and maxima were observed at 0.30-0.35 nm. The hydrogen bonds distribution plot showed that the formation of hydrogen bonds starts at 0.26 nm while the maximum distribution was observed at 0.30-0.35 nm (Fig. 7).

Computation of binding free energy of Gravacridonechlorine-3CLpro complex

Gravacridonechlorine binding strength with 3CLpro was computed in the form of ΔG_{bind} using MMPBSA. The MMPBSA, ΔG_{bind} calculations represent the stable binding between Gravacridonechlorine and the active site of the 3CLpro complex. The contribution to ΔG_{bind} of Gravacridonechlorine-3CLpro complex was made by various energy components like Electrostatic energy (E_{EEL}), ΔG_{npsolv} , ΔG_{psolv} and van der Waals energy (ΔE_{vdw}). ΔE_{vdw} (-162.259 kJ/mol), E_{EEL} (-7.046 kJ/mol),

and SASA energy (-13.379 kJ/mol) contributed to the negative value of the ΔG_{bind} (-134.142 kJ/mol) while the positive values of ΔG_{psolv} (48.542 kJ/mol) were deducted to get the final score through MMPBSA analysis. The negative value of ΔG_{bind} (-134.142 kJ/mol) showed that the Gravacridonechlorine molecule has a high affinity with 3CLpro.

Conclusion

In silico investigations identified Gravacridonechlorine as a potential inhibitor for norovirus 3CLpro. The molecular docking results corroborated with MMPBSA and MD simulation studies. These findings suggest that Gravacridonechlorine, a metabolite derived from the medicinal plant *Ruta graveolens*, could serve as a promising lead compound for the development of novel anti-norovirus therapeutics. Further *in vitro* and *in vivo* studies are warranted to validate these computational predictions and assess the therapeutic potential of Gravacridonechlorine.

Acknowledgement

Authors acknowledge Chaudhary Charan Singh University, Meerut for providing the required facilities to carry out this research work.

Conflicts of interest

All authors declare no conflicts of interest.

References

- 1 Robilotti E, Deresinski S, & Pinsky BA, Norovirus. *Clin Microbial Rev*, 28 (2015) 134.
- 2 Chhabra P, de Graaf M, Parra GI, Chan MC, Green K, Martella V, Wang Q, White PA, Katayama K, Vennem H, Koopmans MPG & Vinjé J, Updated classification of norovirus genogroups and genotypes. *J Gen Virol*, 100 (2019) 1393.

- 3 de Graaf M, van Bee J & Koopmans MP, Human norovirus transmission and evolution in a changing world. *Nat Rev Microbiol*, 14 (2016) 421.
- 4 Ghosh S, Malik YS & Kobayashi N, Therapeutics and Immunoprophylaxis Against Noroviruses and Rotaviruses: The Past, Present, and Future. *Curr Drug Metab*, 19 (2018) 170.
- 5 Omatola CA, Mshelbwala PP, Okolo MO, Onoja AB, Abraham JO, Adaji DM, Samson SO, Okeme TO, Aminu RF, Akor ME, Ayeni G, Muhammed D, Akoh PQ, Ibrahim DS, Edegbro E, Yusuf L, Ocean HO, Akpala SN, Musa OA & Adamu AM, Noroviruses: Evolutionary Dynamics, Epidemiology, Pathogenesis, and Vaccine Advances-A Comprehensive Review. *Vaccines (Basel)*, 12 (2024) 590.
- 6 Ji L, Hu G, Xu D, Wu X, Fu Y & Chen L, Molecular epidemiology and changes in genotype diversity of norovirus infections in acute gastroenteritis patients in Huzhou, China, 2018. *J Med Virol*, 92 (2020) 3173.
- 7 Kankanamalage ACG, Kim Y, Weerawarna PM, Uy RA, Damalanka VC, Mandadapu SR, Alliston KR, Mehzabeen N, Battaile KP, Lovell S, Chang KO & Groutas WC, Structure-guided design and optimization of dipeptidyl inhibitors of norovirus 3CL protease. Structure-activity relationships and biochemical, X-ray crystallographic, cell-based, and *in vivo* studies. *J Med Chem*, 58 (2015) 3144.
- 8 Chang KO, Kim Y, Lovell S, Rathnayake AD & Groutas WC, Antiviral Drug Discovery: Norovirus Proteases and Development of Inhibitors. *Viruses*, 11 (2019) 197.
- 9 Rathnayake AD, Kim Y, Dampalla CS, Nguyen HN, Jesri AM, Kashipathy MM, Lushington GH, Battaile KP, Lovell S, Chang KO & Groutas WC, Structure-Guided Optimization of Dipeptidyl Inhibitors of Norovirus 3CL Protease. *J Med Chem*, 63 (2020) 11945.
- 10 Damalanka VC, Kim Y, GalasitiKankanamalage AC, Rathnayake AD, Mehzabeen N, Battaile KP, Lovell S, Nguyen HN, Lushington GH, Chang KO & Groutas WC. Structure-guided design, synthesis and evaluation of oxazolidinone-based inhibitors of norovirus 3CL protease. *Eur J Med Chem* 143 (2018) 881.
- 11 Yang M, Lee G, Si J, Lee SJ, You HJ & Ko G, Curcumin Shows Antiviral Properties against Norovirus. *Molecules*, 21 (2016) 1401.
- 12 He S, Nahhas AF, Habib AH, Alshehri MA, Alshamrani S, Asiri SA, Alnamshan MM, Helmi N, Al-Dhuayan I, Almulhim J, Alharbi AM, Su D, Kumari A & Rahaman A, Identification of compelling inhibitors of human norovirus 3CL protease to combat gastroenteritis: A structure-based virtual screening and molecular dynamics study. *Front Chem*, 10 (2022) 1034911.
- 13 Mullard A, Biotech R&D spends jumps by more than 15. *Nat Rev Drug Discov*, 15 (2016) 447.
- 14 Benedetto TD, Bagnoli D, Rosati L, Marini O, Sancineto F & Santi LC, New Halogen-Containing Drugs Approved by FDA in 2021: An Overview on Their Syntheses and Pharmaceutical Use. *Molecules*, 27 (2022) 1643.
- 15 Fenical W, Jensen PR, Palladino MA, Lam KS, Lloyd GK & Potts BC, Discovery and development of the anticancer agent salinosporamide A (NPI-0052). *Bioorg Med Chem*, 17 (2009) 2175.
- 16 Shinde PB, Lee YM, Dang HT, Hong J, Lee CO & Jung JH, Cytotoxic bromotyrosine derivatives from a two-sponge association of *Jaspis* sp. and *Poecillastra* sp. *Bioorg Med Chem Lett*, 18 (2008) 6414.
- 17 Gentry CL, Egleton RD, Gillespie T, Abbruscato TJ, Bechowski HB, Hrubby VJ & Davis TP, The effect of halogenation on blood-brain barrier permeability of a novel peptide drug. *Peptides*, 20 (1999) 1229.
- 18 Lucero Y, Matson DO, Ashkenazi S, George S & O'Ryan M, Norovirus: Facts and Reflections from Past, Present, and Future. *Viruses*, 13 (2021) 2399.
- 19 Kumar S, Joshi N, Choudhir G, Sharma S, Tiwari A, Alharbi SA, Alfarraj S & Ansari M.J, Halogenated Secondary Metabolites from Higher Plants: Potent Drug Candidates for Chikungunya Using in silico Approaches. *Pol J Microbiol*, 73 (2024) 207.
- 20 Engvild KC, Chlorine-containing natural compounds in higher plants. *Phytochem*, 25 (1986) 781.
- 21 Gribble GW, A recent survey of naturally occurring organohalogen compounds. *Environ Chem*, 12 (2015) 396.
- 22 Kim S, Thiessen PA, Bolton EE, Chen J, Fu G, Gindulyte A, Han L, He J, He S, Shoemaker BA, Wang J, Yu B, Zhang J & Bryant SH, PubChem Substance and Compound databases. *Nucleic Acids Res*, 44 (2016) D1202.
- 23 Lipinski CA, Lombardo F, Dominy BW & Feeney PJ, Experimental and computational approaches to estimate solubility and permeability in drug discovery and development settings. *Adv Drug Deliv Rev*, 23 (1997) 3.
- 24 Daina A, Michielin O & Zoete V, SwissADME: a free web tool to evaluate pharmacokinetics, drug-likeness and medicinal chemistry friendliness of small molecules. *Sci Rep*, 7 (2017) 42717.
- 25 Dallakyan S & Olson AJ, Small-molecule library screening by docking with PyRx. *Methods Mol Biol*, 1263 (2015) 243.
- 26 O'Boyle NM, Banck M, James CA, Morley C, Vermeersch T & Hutchison GR, Open Babel: An open chemical toolbox. *J Chem Inform*, 3 (2011) 33.
- 27 Pettersen EF, Goddard TD, Huang CC, Couch SS, Greenblatt DM, Meng EC & Ferrin TE, UCSF Chimera visualization system for exploratory research and analysis. *J Comput Chem*, 25 (2004) 1605.
- 28 Trott O & Olson AJ, AutoDock Vina: improving the speed and accuracy of docking with a new scoring function, efficient optimization, and multithreading. *J Comput Chem*, 31 (2010) 455.
- 29 Rauf MA, Zubair S, Azhar A, Ligand docking and binding site analysis with PyMol and AutoDock/Vina. *Int J Basic Appl Sci*, 4 (2015) 168.
- 30 Van Der Spoel D, Lindahl E, Hess B, Groenhof G, Mark AE, Berendsen HJ, GROMACS: fast, flexible and free. *J Comput Chem*, 26 (2005) 1701.
- 31 Schüttelkopf AW & Van Aalten DM, PRODRG: a tool for high-throughput crystallography of protein-ligand complexes. *Acta Crystallogr D Biol Crystallogr*, 60 (2004) 1355.
- 32 Hess B, P-LINCS: A parallel linear constraint solver for molecular simulation. *J Chem Theory Comput*, 4 (2008) 116.
- 33 Hess B, Bekker H, Berendsen HJ & Fraaije J, GEM.LINCS: a linear constraint solver for molecular simulations. *J Comput Chem*, 18 (1997) 1463.
- 34 Berendsen HJ, Postma JV, van Gunsteren WF, DiNola A & Haak JR, Molecular dynamics with coupling to an external bath. *J Chem Phys*, 81 (1984) 3684.
- 35 Tripathi A & Mishra K, Molecular docking: A structure-based drug designing approach. *JSM Chem*, 5 (2017) 1042.

- 36 Konstantinidis K, Karakasiliotis I, Anagnostopoulos K & Boulougouris GC, On the estimation of the molecular inaccessible volume and the molecular accessible surface of a ligand in protein–ligand systems. *Mol Syst Des Eng*, 6 (2021) 946.
- 37 Qaisi AI, Alfarayeh I, Alsarayreh A, Khleifat K & Abu-Nwas N, Assessment of antioxidant potential, cytotoxicity, and anticancer activity of methanolic extracts from selected wild medicinal plants. *Phy Plu*, 4 (2024) 100534.
- 38 Manogar P, Prabhu SV, Durairaj P, Abel MMJ, Prakash N & Jayanthi S, Molecular docking interaction of bioactive molecules from *Kigeliaafricana* (lam.) benth., revealed potential inhibitors of penicillin-binding protein 2 (PBP2). *Mol Aspects Med*, 4 (2024) 100051.
- 39 Grottesi A, Besker N, Emerson A, Manelfi C, Beccari AR, Frigerio F, Lindahl E, Cerchia C & Talarico C, Computational Studies of SARS-CoV-2 3CLpro: Insights from MD Simulations. *Int J Mol Sci*, 21 (2020) 5346.